

# THE K<sup>+</sup> CHANNEL OF SARCOPLASMIC RETICULUM

## A New Look at Cs<sup>+</sup> Block

SAMUEL CUKIERMAN, GARY YELLEN, AND CHRISTOPHER MILLER

*Graduate Department of Biochemistry, Brandeis University, Waltham, Massachusetts*

**ABSTRACT** K<sup>+</sup>-selective ion channels from mammalian sarcoplasmic reticulum were inserted into planar phospholipid bilayers, and single-channel currents measured in solutions containing Cs<sup>+</sup>. Current through this channel can be observed in symmetrical solutions containing only Cs<sup>+</sup> salts. At zero voltage, the Cs<sup>+</sup> conductance is approximately 15-fold lower than the corresponding K<sup>+</sup> conductance. The open channel rectifies strongly in symmetrical Cs<sup>+</sup> solutions, and the Cs<sup>+</sup> currents are independent of Cs<sup>+</sup> concentration in the range 18–600 mM. Biionic (Cs<sup>+</sup>/K<sup>+</sup>) reversal potentials are only 10 mV, showing that Cs<sup>+</sup> is nearly as permeant as K<sup>+</sup>, though much less conductive. Addition of Cs<sup>+</sup> to symmetrical K<sup>+</sup> solutions reduces current through the channel in a voltage-dependent way. The results can be explained by a free energy profile in which the channel's selectivity filter acts in two ways: to provide binding sites for the conducting ions and to serve as a major rate-determining structure. According to this picture, the main difference between high-conductance K<sup>+</sup> and low-conductance Cs<sup>+</sup> is that Cs<sup>+</sup> binds to an asymmetrically positioned site ~20-fold more tightly than does K<sup>+</sup>.

### INTRODUCTION

Virtually all K<sup>+</sup>-selective ion channels interact strongly with Cs<sup>+</sup>. Indeed, there is no known case in which a K<sup>+</sup> channel—that is, an ion channel with a substantial selectivity for K<sup>+</sup> over Na<sup>+</sup>—is not profoundly affected by Cs<sup>+</sup> in the millimolar range. In all cases studied, Cs<sup>+</sup> reduces K<sup>+</sup> current through the open channel, i.e., it blocks the channel. The common mechanistic picture of this interaction is analogous to competitive inhibition in enzyme kinetics: the Cs<sup>+</sup> ion can enter the normal K<sup>+</sup> conduction pathway, but cannot permeate it. Whenever a Cs<sup>+</sup> ion is thus stuck in the open channel, K<sup>+</sup> ions are literally blocked from permeating. K<sup>+</sup> ions must wait for the Cs<sup>+</sup> ion to leave the channel via the same route that it had entered before they can traverse the pore. Though many variations in detail have been offered in the literature of Cs<sup>+</sup> block of K<sup>+</sup> channels, such studies are usually interpreted in terms of these basic elements: the strong binding and nonpermeation of the Cs<sup>+</sup> ion.

This picture is reasonable. A K<sup>+</sup>-selective site of low field strength may easily be expected to bind Cs<sup>+</sup> more strongly than K<sup>+</sup> (Eisenman, 1961). Since Cs<sup>+</sup> is slightly larger than K<sup>+</sup> (0.31 vs. 0.27 nm diameter, respectively), it is plausible to propose that simple steric hindrance accounts for the failure of Cs<sup>+</sup> to permeate the selectivity filter of a K<sup>+</sup> channel.

This study is concerned with Cs<sup>+</sup> block of a K<sup>+</sup>-selective

channel from the sarcoplasmic reticulum (SR), a channel whose ion conduction properties have been extensively studied (Coronado and Miller, 1979; Coronado et al., 1980; Miller et al., 1984). Cs<sup>+</sup> has been shown to reduce K<sup>+</sup> currents through this channel in a particularly simple manner. Cs<sup>+</sup> appears to bind competitively with K<sup>+</sup> at a single site within the channel; the affinity of Cs<sup>+</sup> for this site varies with applied voltage as though the site is located 35% of the way down the voltage drop across the channel. Since Cs<sup>+</sup> is effective as a blocker from only one side of the channel (the *cis* side), and since previous studies failed to detect conduction by Cs<sup>+</sup>, we concluded that this blocker ion is in fact impermeant, and therein lies its ability to inhibit K<sup>+</sup> conduction (Coronado and Miller, 1979).

The fact that Cs<sup>+</sup> blocks the SR K<sup>+</sup> channel is surprising, since it is known (Coronado and Miller, 1982) that organic cations as large as 0.5 nm in diameter can permeate; the smaller Cs<sup>+</sup> ion, then, cannot be excluded from permeating for purely steric reasons. We now show that our previous plug-in-the-bottle picture of Cs<sup>+</sup> block is incorrect, that the Cs<sup>+</sup> permeability is nearly as high as that of K<sup>+</sup>. We also show that a simple picture of Cs<sup>+</sup> conduction through the channel can quantitatively explain all our results on voltage-dependent inhibition of K<sup>+</sup> currents by Cs<sup>+</sup> as well as on open-channel currents under symmetrical Cs<sup>+</sup> and biionic Cs<sup>+</sup>/K<sup>+</sup> conditions.

### MATERIALS AND METHODS

In all experiments here, currents through single channels were recorded by inserting purified SR membrane vesicles into planar lipid bilayers composed of 90% phosphatidylethanolamine/10% phosphatidylcholine.

Dr. Cukierman's permanent address is Instituto de Biofísica, Universidade Federal do Rio de Janeiro, 21941 Rio de Janeiro, Brazil

Preparation of SR vesicles from rabbit skeletal muscle and of phospholipids has been described, as have the methods used to insert  $K^+$  channels into the planar bilayers (Labarca et al., 1980). SR vesicles were added to the *cis* side of the membrane, while the opposite *trans* side is defined as zero voltage. All aqueous solutions used were composed of the  $SO_4^-$  salt of the indicated cation, and also contained 10 mM HEPES neutralized to pH 7.5 with the appropriate cation hydroxide. Single-channel data were recorded on chart paper and were analyzed by hand. Each experiment was repeated in 3–8 separate bilayers. Temperature was 21–23°C.

Only two significant variations over previous studies were used. First, we connected the Ag/AgCl electrodes to the bilayer chambers with salt bridges containing 3M KCl (rather than 0.2 M KCl); the use of lower ionic strength salt bridges gave serious errors (5–10 mV) in the measurement of reversal potentials under mixed-ion conditions. Second, in almost all experiments involving the measurements of  $Cs^+$  currents, we inserted channels into the bilayers in the presence of symmetrical  $K^+$  solutions, and subsequently exchanged these with  $Cs^+$ -containing solutions; in this way, we could confidently identify the channel under study as the SR  $K^+$  channel.

## RESULTS

### $Cs^+$ is a Conducting Ion

In our previous work on ion conduction through the SR  $K^+$  channel (Coronado et al., 1980), we were unable to observe any single-channel conductance fluctuations in the presence of symmetrical  $Cs^+$  solutions. In those studies, we used high concentrations (1–2 M) of  $Cs^+$  in hopes of enhancing any small current that might be present. We now show in Fig. 1 that clear channel fluctuations may be easily observed in symmetrical  $Cs^+$  solutions at lower concentrations, 30 to 300 mM. There are three pieces of evidence (not shown) telling us that the channel observed in symmetrical  $Cs^+$  is in fact the SR  $K^+$  channel. First, the voltage dependence of channel opening is similar in  $K^+$  and  $Cs^+$ ; channel opening is enhanced as voltage is made increasingly positive, and the kinetics of gating are similar. Second, the single-channel  $Cs^+$  currents are inhibited by decamethonium (150  $\mu$ M) on the *trans* side of the channel, as are the corresponding  $K^+$  currents. Finally,  $Cs^+$  current fluctuations as in Fig. 1 were obtained by inserting a single SR channel in symmetrical  $K^+$  and subsequently perfusing both sides of the bilayer with  $Cs^+$  solution.

$Cs^+$  is less conductive in this channel than  $K^+$ ; at zero voltage at 600 mM  $Cs^+$ , the conductance is 15 pS, 16-fold smaller than the corresponding value for  $K^+$ . Two additional properties of the  $Cs^+$  current through single channels are obvious in Fig. 1: open-channel rectification and concentration independence. These characteristics are documented more fully in Fig. 2, which shows the current-voltage relation ( $I$ - $V$  curve) under conditions of symmetrical  $Cs^+$ , at concentrations from 18 to 600 mM. The channel displays rectification: negative (*trans*-to-*cis*)  $Cs^+$  current passes more easily than does positive (*cis*-to-*trans*) current. Most remarkable is the fact that the  $I$ - $V$  curves are identical over an enormous range of  $Cs^+$  concentrations, from 18 to 600 mM. Since we know (Coronado et al., 1980) that for the other alkali metal cations the channel saturates with ion concentration, we conclude that the  $Cs^+$  conductance is already saturated by 18 mM. It was not possible to collect data at  $Cs^+$  concentrations lower than 15 mM, as channel opening becomes very rare under these conditions.

### $Cs^+$ is Nearly as Permeant as $K^+$

The results above show that  $Cs^+$  is much less conductive than  $K^+$  through the SR  $K^+$  channel. An alternative measurement of ionic selectivity is the reversal potential under biionic conditions, i.e., the zero-current voltage,  $\Psi_o$ , measured with  $Cs^+$  on one side of the bilayer and  $K^+$  at the same concentration on the other. The ratio of the two ion permeabilities is defined by the reversal potential:

$$P_{Cs}/P_K = \exp(-F\Psi_o/RT). \quad (1)$$

As discussed by Hille (1975a), these two measurements of ion selectivity, conductance and permeability, do not in general agree, since they are expressions of different rate processes in the channel permeation mechanism. Under biionic conditions (Fig. 3), the SR  $K^+$  channel shows high permeability to  $Cs^+$ , nearly as high as to  $K^+$ . The biionic reversal potential is only 10 mV, indicating a  $P_{Cs}/P_K$  of 0.7.



FIGURE 1 Single SR  $K^+$  channels in symmetrical  $Cs^+$  solutions. Channels were inserted into planar bilayers as described in Methods, in the presence of symmetrical  $K^+$  solutions. Immediately after appearance of channels, both sides of the bilayer were extensively perfused with  $Cs^+$  solutions at the indicated concentrations. Records were then collected at holding voltages shown. In all traces, channel opening is upward.

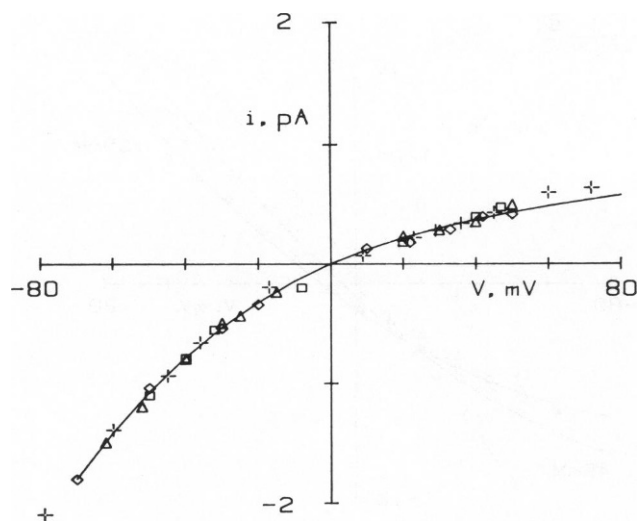


FIGURE 2 Current-voltage curve in symmetrical  $\text{Cs}^+$ . Single-channel currents were measured as a function of voltage in symmetrical solutions of the following  $\text{Cs}^+$  concentrations: (+) 18 mM, (□) 50 mM, (◇) 300 mM, (Δ) 600 mM. Solid curve is drawn according to the model of Fig. 5, using the parameters of Table I; virtually identical curves are obtained from the model of Fig. 6 and parameters of Table II. The curve here is drawn for a  $\text{Cs}^+$  concentration of 50 mM, but identical curves are obtained over entire range of  $\text{Cs}^+$  concentrations from 20 to 600 mM.

The  $I$ - $V$  curves of Fig. 3 also show that this value is independent of the absolute concentration of salt, as expected for a single-ion channel such as this (Coronado et al., 1980). The permeability ratio is the same regardless of the polarity of the biionic conditions, but the shapes of the  $I$ - $V$  curves are different with  $\text{Cs}^+$  on the *cis* side than with  $\text{Cs}^+$  on the *trans* side, as expected from the rectification of the pure  $\text{Cs}^+$  currents; positive  $\text{Cs}^+$  current is more difficult to drive through this channel than is negative  $\text{Cs}^+$  current.

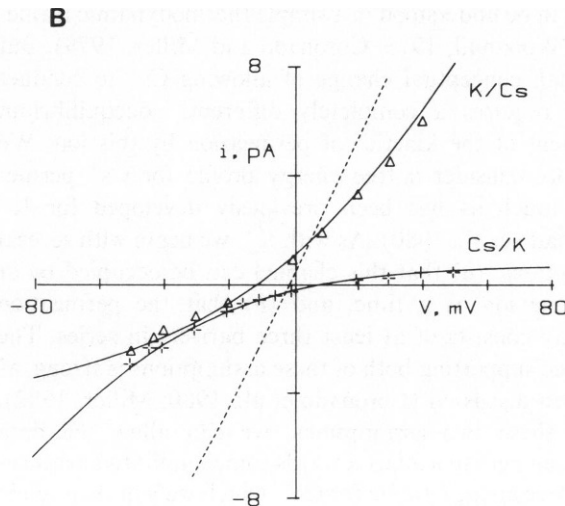
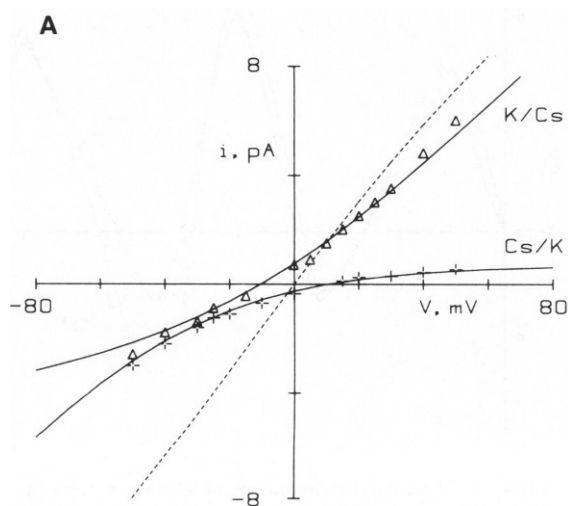


FIGURE 3  $I$ - $V$  curves for  $\text{K}^+/\text{Cs}^+$  biionic conditions. Current-voltage curves were collected for channels under biionic conditions, with  $\text{Cs}^+$  on the *cis* side and  $\text{K}^+$  on the *trans* ( $\text{Cs}/\text{K}$ ), or with the ions reversed ( $\text{K}/\text{Cs}$ ). Cation concentrations were 50 mM (A) or 300 mM (B). Solid curves drawn as in Fig. 2. Dashed  $I$ - $V$  curves were obtained for symmetrical  $\text{K}^+$  at the appropriate concentration, and data points are omitted for clarity.

## $\text{Cs}^+$ Blocks $\text{K}^+$ Currents under Mixed-Ion Conditions

Having established that  $\text{Cs}^+$  does permeate the SR  $\text{K}^+$  channel, we now address the question of  $\text{Cs}^+$  blocking of  $\text{K}^+$  currents. In Fig. 4 we illustrate a series of classical blocking experiments: the addition of  $\text{Cs}^+$  to one side of a membrane separating identical  $\text{K}^+$  solutions. As found previously (Coronado and Miller, 1979; Coronado et al., 1980), addition of  $\text{Cs}^+$  to the *cis* side of the bilayer reduces  $\text{K}^+$  currents. The effect is voltage dependent; block is strong at positive voltages and is relieved as voltage is made increasingly negative.  $\text{Cs}^+$  added to the *trans* side has a much smaller blocking effect, although a discernable one. Results like this had previously been taken as evidence that  $\text{Cs}^+$  binds to a site ~40% of the way through the voltage gradient, from the *cis* side of the membrane (Coronado and Miller, 1979), and we will see that in spite of the fact that we now know that  $\text{Cs}^+$  is permeant, this conclusion still holds.

## DISCUSSION

The major finding of this study is that  $\text{Cs}^+$ , which we had previously considered an impermeant blocker of the SR  $\text{K}^+$  channel, is in fact a conducting ion. We would like to gain a quantitative view of the conduction by  $\text{Cs}^+$  through this channel and to consider what new light these results shed upon the structural picture that has already been derived of its conduction pathway.

## $\text{Cs}^+$ Conduction and Block

Qualitatively, it is a simple task to account for  $\text{Cs}^+$  block of  $\text{K}^+$  currents concomitant with  $\text{Cs}^+$  conduction. Whereas the usual picture of  $\text{Cs}^+$  block, which we had adopted

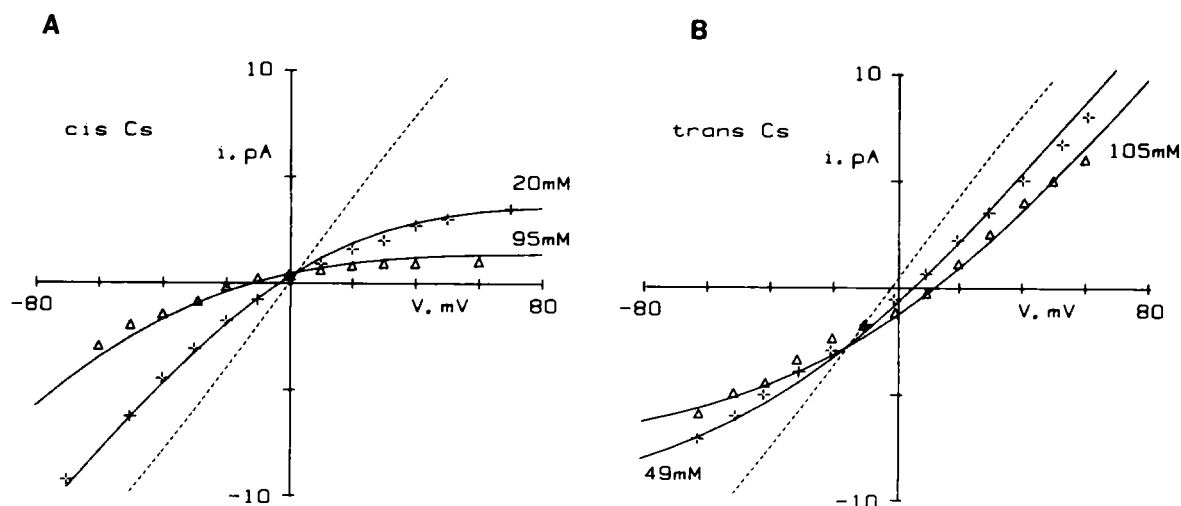


FIGURE 4  $\text{Cs}^+$  blocking curves. Single-channel currents were measured in solutions of symmetrical  $\text{K}^+$ , 300 mM, with the indicated concentration of  $\text{Cs}^+$  added to one side. (A)  $\text{Cs}^+$  added to *cis* side. (B)  $\text{Cs}^+$  added to *trans* side. Dashed  $I$ - $V$  curves were obtained without added  $\text{Cs}^+$  (for clarity, data points are omitted). Solid curves are drawn as in Fig. 2.

previously, states that  $\text{Cs}^+$  binds to but cannot traverse the channel, we can now simply say that  $\text{Cs}^+$  binds and can permeate, albeit with low conductance. This picture of low-conductance permeant-ion blocking has been documented with conducting ions in  $\text{Na}^+$  channels (Hille, 1975b), in squid axon  $\text{K}^+$  channels (French and Wells, 1977), in the acetylcholine-activated channel of end plate (Lewis, 1979; Adams et al., 1981), and in  $\text{Ca}^{++}$  channels (Hess and Tsien, 1984). According to this view, as  $\text{Cs}^+$  is added to solutions containing symmetrical  $\text{K}^+$ , the occupancy of the channel by  $\text{Cs}^+$  increases, and the total current becomes increasingly dominated by the low-conductance  $\text{Cs}^+$  ion at the expense of the high-conductance  $\text{K}^+$  ion.

We now approach this idea quantitatively. In a theory considering  $\text{Cs}^+$  as nonconducting, the block of  $\text{K}^+$  currents can be understood in a simple thermodynamic framework (Woodhull, 1973; Coronado and Miller, 1979). But the small conceptual change of allowing  $\text{Cs}^+$  to conduct slowly requires a completely different, nonequilibrium treatment of the kinetics of permeation by this ion. We therefore consider a free energy profile for  $\text{Cs}^+$  permeation, much as has been previously developed for  $\text{K}^+$  (Coronado et al., 1980). As with  $\text{K}^+$ , we begin with several assumptions: (a) that this channel can be occupied by at most one ion at a time, and (b) that the permeation pathway consists of at least three barriers in series. The evidence supporting both of these assumptions is strong, as has been discussed (Coronado et al., 1980; Miller, 1982). Using these two assumptions, we can allow the data presented here to lead us towards some qualitative features of the free energy profile for  $\text{Cs}^+$ , which we will then refine quantitatively to arrive at the final workable conduction model illustrated in Fig. 5.

The first pertinent facts are apparent from the  $I$ - $V$  curve in symmetrical  $\text{Cs}^+$  (Fig. 2). We see that these curves are

utterly independent of  $\text{Cs}^+$  concentration in the range 20–600 mM. We conclude that the channel is saturated with  $\text{Cs}^+$  at all these concentrations, and that therefore the dissociation constant of  $\text{Cs}^+$  for the channel (at zero voltage) is  $<5$  mM. Since the dissociation constant is an expression of the energy wells only (Läuger, 1973; Hille, 1975a), we can say that the well depth of the  $\text{Cs}^+$  binding sites is  $-5.3 RT$  or lower. We note further that the conductance for  $\text{Cs}^+$ , which is the maximum, or saturation level, conductance for this ion, is 10–20-fold lower than for  $\text{K}^+$ . This tells us that the rate-limiting barrier to  $\text{Cs}^+$  exit from the channel is  $\sim 3 RT$  larger than that for  $\text{K}^+$  (Coronado et al., 1980). An additional consideration is that

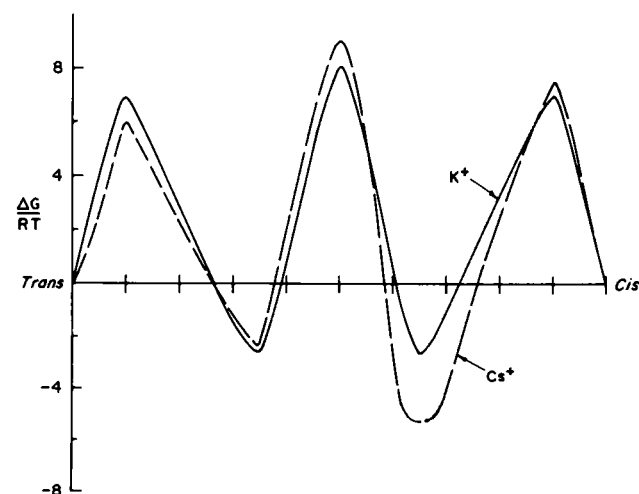


FIGURE 5 Three-barrier free energy profiles for  $\text{K}^+$  and  $\text{Cs}^+$ . The  $I$ - $V$  curves were fit by eye using parameters for a three-barrier, two-site single-ion conduction model, as previously described for this channel (Coronado et al., 1980). Barriers were positioned symmetrically, with wells constrained at electrical distances of 0.38 and 0.62. Parameters are given in Table I.

the  $\text{Cs}^+/\text{K}^+$  permeability ratio, which is an expression of the differences only in the peak energies (Hille, 1975a; Coronado et al., 1980), is close to unity. Thus, the  $\text{Cs}^+$  peak energies cannot be much larger than those for  $\text{K}^+$ .

The  $\text{Cs}^+$  conduction pathway is clearly asymmetric, as shown both by the sidedness of  $\text{Cs}^+$  blocking action and the  $I$ - $V$  curve rectification in symmetrical  $\text{Cs}^+$ . These characteristics imply that the *cis*-facing  $\text{Cs}^+$  binding site is substantially deeper than the *trans*-facing site and that the barrier for  $\text{Cs}^+$  leaving this site towards the *cis* side is smaller than that for leaving the site toward the *trans* side. Qualitatively, then, we conclude that the  $\text{Cs}^+$  conduction profile displays a *cis*-facing well that is deeper than the *trans*-facing well by 3–4  $RT$ , and deeper by the same amount than the corresponding wells for  $\text{K}^+$ ; the peak energies for  $\text{Cs}^+$  are about the same as for  $\text{K}^+$ .

We can refine the gross features of this model by using the free energy profiles of  $\text{K}^+$  and  $\text{Cs}^+$  to fit all the data presented here. We take the rate constant,  $k_i$ , over each barrier of energy  $\Delta G_i^*$  to be given by:

$$k_i = \nu \exp(-\Delta G_i^*/RT). \quad (2)$$

The six linear flux equations (three each for  $\text{K}^+$  and  $\text{Cs}^+$ ) may then be solved for the currents as a function of voltage, by a method described previously (Begenisich and Cahalan, 1980). In the treatment here, the preexponential factor,  $\nu$ , is entirely arbitrary as long as it is kept the same for both ions; we assign it a value of  $kT/h$  (equivalent to  $\sim 10^6$  pA), to be consistent with previous work on this channel (Coronado et al., 1980). We have used this approach to model ionic conduction under symmetrical (Fig. 2), biionic (Fig. 3), and mixed ionic (Fig. 4) conditions and have adjusted parameters to achieve satisfactory fits to all the data (solid curves in all figures). Fig. 5 displays our final free energy profiles, and Table I reports values of the parameters used in these profiles.

The remarkable conclusion of Fig. 5 is that the profiles for both  $\text{Cs}^+$  and  $\text{K}^+$  are very nearly the same, except for a single feature: the deep *cis*-facing well for  $\text{Cs}^+$ , positioned at an electrical distance of 0.38 (i.e., 38% of the way down

the voltage drop from the *cis* side). The position of this well is very tightly determined by the  $\text{Cs}^+$  blocking data (Fig. 5); we cannot fit the voltage dependence of  $\text{Cs}^+$  block without assuming that this site is located between 0.34 and 0.40 electrical distance. The depth of this well almost wholly accounts for the 15–20-fold difference in  $\text{Cs}^+$  vs.  $\text{K}^+$  conductance, while the slightly higher central peak accounts for the  $\text{Cs}^+$  rectification (Fig. 2). This well depth is not subject to much variation, given the constraints of our data. If it were shallower, the  $\text{Cs}^+$  dissociation constant would be too large, and we would observe  $I$ - $V$  curves that vary with  $\text{Cs}^+$  concentration; the lack of such variation (Fig. 2) means that the well depth must be below  $-5.3 RT$ . However, the well cannot be deeper than  $-6 RT$ , or else the  $\text{Cs}^+$  conductance at zero voltage would be much lower than is actually measured.

The  $\text{Cs}^+$  dissociation constant predicted from this free energy profile is 3.5 mM. This value is too low for us to observe directly as a variation of  $\text{Cs}^+$  conductance with concentration, since it is very difficult to obtain channel fluctuations at salt concentrations lower than 15 mM. But we can estimate this value independently, assuming that this is a single-ion channel in which the peak-height differences between  $\text{K}^+$  and  $\text{Cs}^+$  are not large. In this case, it can be shown (Coronado et al., 1980) that:

$$K_{\text{Cs}} = K_{\text{K}}[\gamma_{\text{Cs}}^{\text{max}}/\gamma_{\text{K}}^{\text{max}}][P_{\text{K}}/P_{\text{Cs}}]. \quad [3]$$

All the parameters on the right side of Eq. 3 are known ( $K_{\text{K}} = 54$  mM;  $\gamma_{\text{K}}^{\text{max}} = 240$  pS;  $\gamma_{\text{Cs}}^{\text{max}} = 15$  pS;  $P_{\text{Cs}}/P_{\text{K}} = 0.67$ ) from this and other work (Coronado et al., 1980). The calculated value of  $K_{\text{Cs}}$  is 5 mM, in good agreement with 3.5 mM estimated from the free energy profile fits.

As with the  $\text{Cs}^+$  well depth and position, most of the parameters in the permeation profile are closely determined by the data. With this three-barrier model, the *trans*-facing well must be symmetrically positioned, i.e., at 0.6 electrical distance, since the  $I$ - $V$  curves for symmetrical  $\text{K}^+$  are nearly linear up to 100 mV of either polarity (Coronado et al., 1980). Similarly, variations in the central and *cis*-facing peaks for  $\text{Cs}^+$  lead to serious departures of the calculated  $I$ - $V$  curves from the data. Only the *trans*-facing  $\text{Cs}^+$  peak is not well determined by the data; it cannot be made higher without compromising the  $I$ - $V$  curves, but it could be made lower.

TABLE I  
SYMMETRICALLY PLACED  
THREE-BARRIER MODEL

$\delta$	Energy [ $\text{K}^+$ ]	Energy [ $\text{Cs}^+$ ]
0.1	7.0	7.2
0.4	-2.7	-5.6
0.5	8.1	8.9
0.6	-2.7	-2.3*
0.9	7.0	6.0

Parameters for free energy profiles depicted in Fig. 5. The table reports the free energy values (in  $RT$  units) at the given electrical distance,  $\delta$ , for  $\text{K}^+$  and  $\text{Cs}^+$ . Asterisk marks parameter that can be varied up to 1  $RT$  unit without affecting fits to the data. Solid curves in Figs. 2, 3, and 4 are drawn according to this model.

### Pore Structure and a More Realistic Energy Profile

On the basis of previous work, we now have a self-consistent picture of the permeation pathway of the SR  $\text{K}^+$  channel (reviewed by Miller et al., 1984). The entire free energy profile is viewed as packed into a short tunnel about 1 nm in length, as in Fig. 6. This tunnel is, for most of its length,  $\sim 0.8$  nm in diameter, but at a point 35–40% of the way down the voltage drop, the tunnel narrows to 0.4–0.5 nm in width. Unfortunately, the three-barrier free energy

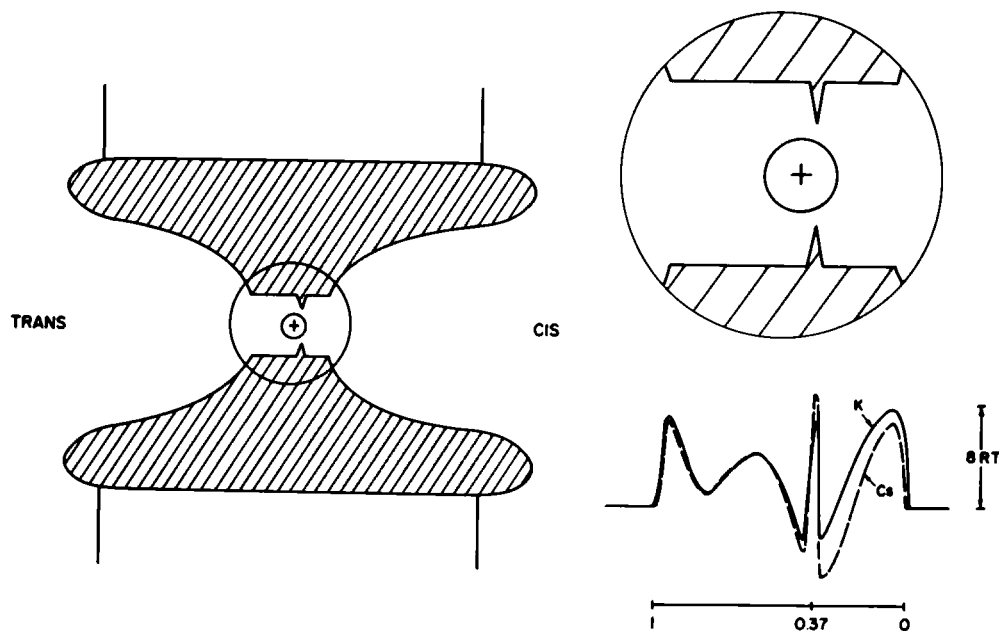


FIGURE 6 Pore structure and a four-barrier model. A scheme is drawn of the physical model previously derived for this channel (Miller, 1982; Miller et al., 1984) on the basis of conduction and blocking studies. An enlargement of the tunnel region, along which the applied voltage is proposed to drop, is shown in register with free energy profiles for  $K^+$  (solid) and  $Cs^+$  (dashed). These profiles were derived by fitting the  $I$ - $V$  data to the model, with parameters given in Table II. The unhydrated  $Cs^+$  ion shown in the scheme is drawn to scale.

profiles derived above for the conducting ions are not consistent with this structure. The main problem concerns the symmetry of the channel. On one hand, the channel's diffusion pathway is clearly asymmetric in structure; both  $Cs^+$  and organic cations (Coronado and Miller, 1982) block at a specific binding site at an electrical distance of  $\sim 0.4$ . But on the other hand, the free energy profile derived for  $K^+$  is highly symmetric, with three energy barriers symmetrically positioned along the pore. It makes sense that the blocking site for organic cations and  $Cs^+$  should be located near the constricted region of the channel, the selectivity filter. But why should there be a second barrier for  $K^+$  movement in the middle of the wider tunnel region? Furthermore, why should a blocker's binding site be located near the selectivity filter, which should be an energy peak in the channel (Armstrong, 1975)?

Of course, without a detailed structure of this channel protein, we cannot answer these questions. But we do wish to propose an alternative ion conduction profile which is more harmonious with our structural picture of this pore. This profile, shown in Fig. 6, is highly asymmetric. We propose, as Hille (1975b) has done for the  $Na^+$  channel, that the selectivity constriction itself provides both ion binding sites and a major rate-determining step for transport through the channel. We imagine that a cluster of polar groups is located at the selectivity filter, and that a conduction ion can approach this structure from either side and bind to it before being fully liganded in the center of the hole. The configuration in which an ion is complexed with the selectivity filter in front and water behind is proposed to represent a binding well in the free energy

profile. There will be two of these, one for approach from the left, and one from the right. We further postulate that the really difficult step for the conducting ion is the actual transit through the selectivity filter, i.e., in moving between leftward and rightward binding positions. It is reasonable to suppose that this step might be energetically unfavorable, since additional dehydration of the ion will have to occur here, concomitant with specific liganding by the groups in the selectivity filter.

Our pore thus contains an active site, with a single liganding structure in the channel contributing two binding sites and a transition state. We place these close together, at electrical distances of 0.34, 0.37, and 0.4, to be consistent with the voltage dependences of both organic and inorganic blockers. The pore should also contain barriers to entry, since partial dehydration will occur when the conducting ion enters the 0.8 nm-wide tunnel region; accordingly, we place barriers at electrical distances of 0.05 and 0.95, respectively. Once an ion enters the tunnel from the *trans* side by hopping over the barrier at 0.95 electrical distance, what does it experience? According to our structural picture, it will diffuse along a relatively wide, featureless region until encountering the constriction. We envision this relatively free diffusion process as a series of small energy barriers, and for simplicity we model this as a single low barrier. This is not an entirely unreasonable assumption, given that the distance from the *trans*-facing tunnel entry to the selectivity constriction is only 0.6–0.7 nm (Miller, 1982).

Does the free energy profile thus developed qualitatively, and shown in Fig. 6, work? With the parameters

TABLE II  
ASYMMETRIC FOUR-BARRIER MODEL

$\delta$	Energy [K <sup>+</sup> ]	Energy [Cs <sup>+</sup> ]
0.05	7.6	6.6
0.34	-2.4	-5.4
0.37	7.7	8.8
0.40	-2.5	-3.4
0.60	5*	5*
0.80	0*	0*
0.95	7.0	6.7

Parameters for the four-barrier model of Fig. 6, as in Table II. Asterisks denote parameters that may be varied up to 1  $RT$  unit without affecting the fits to the data.  $I$ - $V$  curves drawn according to this free energy profile are indistinguishable from those drawn in Figs. 2, 3, and 4.

presented in Table II it does. The curves through all the data points shown in this report can be equally well fit by this four-barrier model as with the symmetric three-barrier model. Even the nearly linear  $I$ - $V$  curve for symmetrical K<sup>+</sup>, which was the original reason for choosing a symmetrical energy profile (Coronado et al., 1980), can be well fit with the asymmetric profile here. For the same reasons as with the simpler three-barrier model, the parameters are rather tightly constrained by our data, especially those associated with the positions and energies of the wells and peak at the selectivity filter. This is admittedly a more complicated model than the symmetrical three-barrier proposal, but now the energy profile is consistent with the structural profile of the channel deduced from previous work.

The same qualitative conclusions derived above for the simpler profile still hold. Cs<sup>+</sup> block is a result of tight binding ( $K_D \sim 3$  mM) at the *cis*-facing well, located at 0.34 electrical distance. The peak energies for Cs<sup>+</sup> and K<sup>+</sup> are approximately equal. We would say that the major determinant of ion selectivity in this channel is a three-way interaction of the ion with a single liganding structure in a region 0.4–0.5 nm wide. This structure acts both as a favorable liganding region and an unfavorable rate-limiting selectivity filter, according to the specific position of the ion with respect to the groups in the constriction.

## CONCLUSIONS

The present results resolve the difficulty alluded to in the introduction: the fact that Cs<sup>+</sup> blocks this channel at all. We now know that Cs<sup>+</sup> blocks the channel by binding tightly at a deep well asymmetrically positioned in the permeation pathway, not by plugging up the pathway sterically. The selectivity filter of the channel is wide enough (0.4–0.5 nm) to allow passage of Cs<sup>+</sup>; the low conductance of this ion is simply due to its extremely tight binding. In the framework of our model, we can also assign a full selectivity sequence of monovalent cation binding to the Cs<sup>+</sup> blocking site, by combining our results here with those previously obtained with the other group 1A cations

(Coronado et al., 1980). Equilibrium binding affinity to this site increases in the sequence: K<sup>+</sup>(1)  $\sim$  Rb<sup>+</sup>(1.2)  $<$  Na<sup>+</sup>(1.6)  $<$  Li<sup>+</sup>(2.8)  $<$  Cs<sup>+</sup>(20).

Finally, we ask why we failed to observe Cs<sup>+</sup> currents previously. Our error was due to the fact that in past work (Coronado et al., 1980) we employed very high Cs<sup>+</sup> concentrations ( $>1$  M) to search for the channel. We now know that at high Cs<sup>+</sup>, the channel remains open all the time; no fluctuations can be observed because it simply never closes. This behavior is intimated in the traces of Fig. 1, which show longer open times at 300 mM Cs<sup>+</sup> than at 30 mM Cs<sup>+</sup>. Indeed, we could not obtain Cs<sup>+</sup> data at concentrations higher than 600 mM. The reason for this effect is not known with certainty, but preliminary experiments (not shown) suggest that the channel is able to close only when it is not occupied by an ion. In other words, ion occupancy holds the channel open, as has been suggested for invertebrate acetylcholine receptors (Marchais and Marty, 1979) and squid axon K<sup>+</sup> channels (Swenson and Armstrong, 1982), and indeed for this channel in the presence of various blocking ions (Coronado and Miller, 1982). For a Cs<sup>+</sup> dissociation constant of 3 mM, the channel would be unoccupied only 0.3% of the time at 1 M Cs<sup>+</sup>, and would thus have very little opportunity to close. Single-channel fluctuations at 1 M K<sup>+</sup> could be seen, however, since K<sup>+</sup> binding is 20-fold weaker than that of Cs<sup>+</sup>.

On balance, we are probably grateful to Dr. C. F. Stevens for suggesting the initial experiment the result of which forced us to undertake this study.

This work was supported by National Institutes of Health grant RO1-AM-19826. Dr. Yellen is a Hoffmann-LaRoche fellow of the Life Sciences Research Foundation.

## REFERENCES

- Adams, D. J., W. Nonner, T. M. Dwyer, and B. Hille. 1981. Block of endplate channels by permeant cations in frog skeletal muscle. *J. Gen. Physiol.* 78:593–615.
- Armstrong, C. M. 1975. Potassium pores of nerve and muscle membranes. In *Membranes, a Series of Advances*. G. Eisenman, editor. Vol. 3. 325–358.
- Begenisich, T. B., and M. D. Cahalan. 1980. Sodium channel permeation in squid axon. II. Non-independence and current-voltage relations. *J. Physiol. (Lond.)* 307:243–257.
- Coronado, R., and C. Miller. 1979. Voltage-dependent caesium blockade of a cation channel from fragmented sarcoplasmic reticulum. *Nature (Lond.)* 280:807–810.
- Coronado, R., and C. Miller. 1982. Conduction and block by organic cations in a K<sup>+</sup>-selective channel from sarcoplasmic reticulum incorporated into planar bilayer membranes. *J. Gen. Physiol.* 79:529–547.
- Coronado, R., R. L. Rosenberg, and C. Miller. 1980. Ionic selectivity, saturation, and block in a K<sup>+</sup>-selective channel from sarcoplasmic reticulum. *J. Gen. Physiol.* 76:425–453.
- Eisenman, G. 1961. On the elementary atomic origin of equilibrium ion specificity. In *Symposium on Membrane Transport and Metabolism*. A. Kleinzeller and A. Kotyk, editors. Academic Press Inc., New York. 163–179.
- French, R. L., and J. B. Wells. 1977. Sodium ions as blocking agents and

- charge carriers in the potassium channel of the squid giant axon. *J. Gen. Physiol.* 70:707-724.
- Hess, P., and R. W. Tsien. 1984. Mechanism of ion permeation through calcium channels. *Nature (Lond.)*. 309:453-456.
- Hille, B. 1975a. Ionic selectivity of Na and K channels of nerve membranes. In *Membranes, a Series of Advances*. G. Eisenman, editor. Marcel Dekker Inc., New York. 255-323.
- Hille, B. 1975b. Ionic selectivity, saturation, and block in sodium channels. A four-barrier model. *J. Gen. Physiol.* 66:535-560.
- Labarca, P., R. Coronado, and C. Miller. 1980. Thermodynamic and kinetic studies of the gating behavior of a K<sup>+</sup>-selective channel from the sarcoplasmic reticulum membrane. *J. Gen. Physiol.* 76:397-424.
- Läuger, P. 1973. Ion transport through pores: a rate-theory analysis. *Biochim. Biophys. Acta*. 311:423-441.
- Lewis, C. 1979. Ion concentration dependence of the reversal potential and the single channel conductance of ion channels at the frog neuromuscular junction. *J. Physiol. (Lond.)*. 286:417-445.
- Marchais, D., and A. Marty. 1979. Interaction of permeant ions with channels activated by acetylcholine in *Aplysia* neurones. *J. Physiol. (Lond.)*. 297:9-45.
- Miller, C. 1982. Feeling around inside a channel in the dark. In *Transport in Biomembranes: Model Systems and Reconstitution*. R. Antolini, A. Gliozzi, and A. Gorio, editors. Raven Press, New York. 99-108.
- Miller, C., J. E. Bell, and A. M. Garcia. 1984. The K<sup>+</sup> channel of sarcoplasmic reticulum. *Curr. Top. Membr. Transp.* 21:99-132.
- Swenson, R. P., and C. M. Armstrong. 1981. K<sup>+</sup> channels close more slowly in the presence of external K<sup>+</sup> and Rb<sup>+</sup>. *Nature (Lond.)*. 291:427-429.
- Woodhull, A. 1973. Ionic blockage of sodium channels in nerve. *J. Gen. Physiol.* 61:687-708.